Optoelectronics Research Centre
University of Southampton

Southampton SO17 1BJ, UK
Telephone: +44 1703 593150
e-mail: light@orc.soton.ac.uk

Optical Pulse Compression in Fibre Bragg Gratings

N.G.R.Broderick, D.Taverner, D.J.Richardson, M.Ibsen and R.I.Laming

Abstract

We report the first experimental demonstration of the optical pushbroom - a novel type of all-optical pulse compression. In the optical pushbroom high intensity pump pulses, tuned well away from the resonance of a Bragg grating, modify the transmission of a weak probe tuned near to the grating's photonic bandgap. The clarity of the experimental results and their close agreement with numerical simulations highlight the tremendous potential of the fiber environment for the detailed study and practical application of nonlinear Bragg grating effects.

Recent experiments on nonlinear effects in Bragg gratings have concentrated on self-phase modulation (SPM) effects[1, 2], i.e. the ability of a strong optical beam to instantaneously alter the local refractive index and thus affect its own propagation. In a Bragg grating SPM results in the transmission being bistable with one state (high power) having a transmission of unity while in the other (low power) the transmission is vanishingly small[3]. For strong optical pulses this behaviour can result in all-optical switching. However a major drawback for observing nonlinear behaviour is that the power requirements are severe, especially in optical fibres, due to the low nonlinearity of silica.

An alternative approach to observing nonlinear behaviour in Bragg gratings is to use the cross-phase modulation (XPM) of a strong pump to alter the refractive index seen by a weak probe thus changing the detuning of the probe from the center of the photonic band gap. Although the power requirements are similar to those for self-switching, the advantage of XPM arises as the frequencies of the pump and probe can be widely dis-similar. This allows the pump frequency to be chosen so as to maximize the power available. The probe frequency is then determined by other considerations thus ensuring optimal switching.

The all-optical switching of a fibre Bragg Grating (FBG) was first seen by LaRochelle et al. in 1990[4] using a self-written grating centered at 514nm. In their experiment the probe beam was centered on the grating, while the pump beam had a wavelength of 1064nm. They observed an increase in transmission from 50% to 54% in the presence of the pump. LaRochelle's experiments remain to date the only work done on XPM in Bragg gratings.

Since LaRochelle's work considerable theoretical effect has gone into developing a detailed understanding of XPM in FBGs[5, 6]. This work has focused on the optical pushbroom which is demonstrated here for the first time. Unlike the all-optical switching described above, which is a continuous wave effect, the optical pushbroom requires a strong pump pulse as it relies on the frequency shift of the probe induced by the intensity gradient of the pump through XPM. As the optical pushbroom has been described in detail before[5] a short description here will suffice.
To understand the optical pushbroom it is necessary to first recall the linear properties of a Bragg grating[7]. A Bragg grating reflects strongly over a narrow frequency range centered at the Bragg frequency and strongly affects the propagation of light near this region. Fig. 1 shows the dispersion relationship for light at frequencies close to the bandgap of a grating. Note that the group velocity, given by the slope of the dispersion relation, falls to zero at the band-edge and is a strong function of the frequency. Far from the bandgap the dispersion relationship approaches

that of a uniform medium, indicated by the dashed line in Fig. 1. The curvature of the dispersion relation determines the group velocity dispersion (GVD) of the grating which is many orders of magnitude higher than that of standard optical fibre[7]. Linked to the reduced group velocity is the fact that the electric field inside the grating is significantly higher than the incident or transmitted fields; allowing a large amount of energy to be stored in the Bragg grating[8].

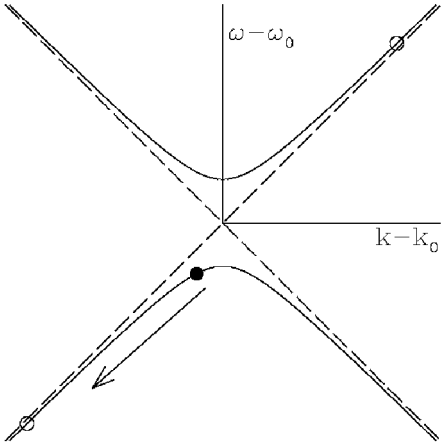

Figure 1: The dispersion relation for a uniform Bragg grating (solid line). The dashed line shows the dispersion relation for a uniform fibre. In our experiment the probe's initial frequency is given by the solid circle and its frequency shift is indicated by the arrow. The two open circles indicate possible locations for the pump beam, which is unaffected by the grating.

The optical pushbroom utilizes these properties by situating a CW probe close to the bandgap where the group velocity is close to zero - one possible frequency is indicated by the solid circle in Fig. 1. When the pump is incident upon the grating, light at the back of the probe ``sees" the pump first and via XPM its frequency is lowered. Thus at any instant there is a frequency chirp across the probe and this chirp combined with the GVD compresses the probe. Furthermore as the frequency of the probe changes it speeds up allowing the back of the probe to sit on the leading edge of the pump where it experiences the maximum XPM for the greatest possible length of time[6]. This process continues along the length of the grating with more and more of the probe's energy being swept up onto the leading edge of the pump.

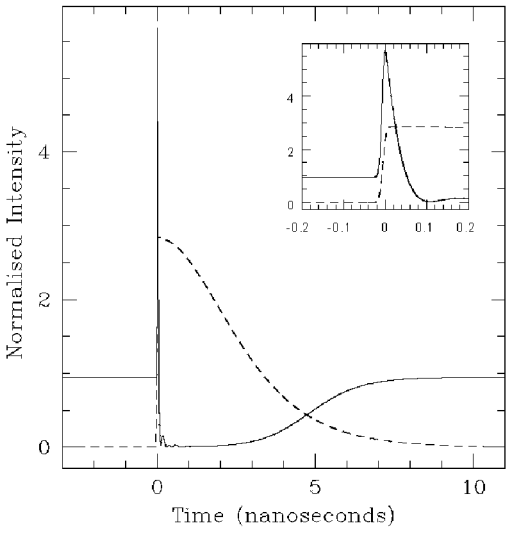

Figure 2: Theoretical trace of the optical pushbroom. The solid line is the transmitted probe intensity, while the dashed line shows the pump profile. The insert is a blowup of the front spike in the transmission. The parameters chosen match those used in the actual experiment.

In transmission one would then expect to see a narrow peak containing a significant fraction of the energy stored in the grating followed by

long dip while the CW field distribution in the grating is restored. These features can be clearly seen in Fig. 2 which shows the results of a numerical simulation of the optical pushbroom for system parameters matched to those of our experiment as detailed below. The solid line gives the probe's intensity as a function of time while the dashed line indicates the pump's profile - on a different vertical scale. The probe's input intensity was normalized to unity and the transmitted intensity prior to the pump gives the linear transmission for this frequency. The insert shows an expanded view of the spike in transmission which has a FWHM of approximately 50ps.

The optical pushbroom illustrates the advantages of using Bragg gratings for nonlinear experiments. The large dispersion of a Bragg grating combined with the resonant field structure allow nonlinear effects to be seen in short lengths (<10cm) of optical fibre. Nonuniform Bragg gratings can also be written in fibres allowing large spatial variations in the dispersion over very short length scales. Theoretical work utilizing these facts have highlighted the possibility of seeing enhanced 2nd harmonic generation[9] amongst other effects. It is perhaps not surprising that Bragg gratings have been described as an ideal soliton environment[10].

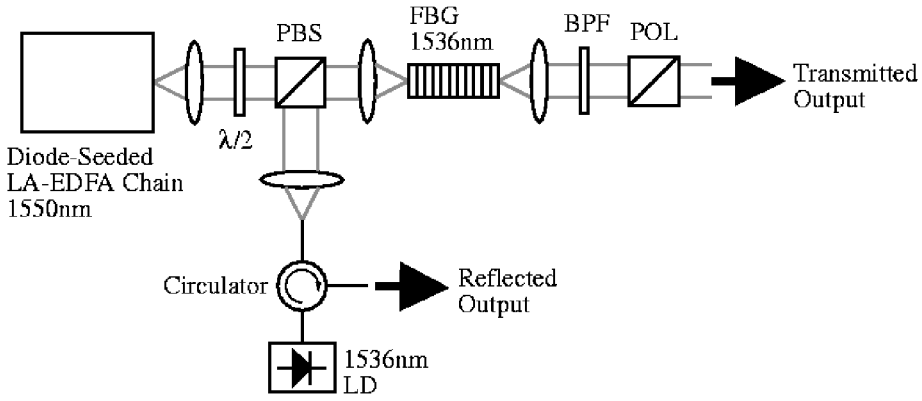

Figure 3: Schematic of the experimental setup. PBS: polarization beam splitter. BPF: bandpass filter with a width of 1nm. LA-EDFA: Large mode area Erbium fibre amplifier. The polarizer (POL) is set to minimize the pump. See the text for more details.

Experimental Results

Our experimental setup is shown in Fig. 3. High power pump pulses at 1550nm are used to switch a low-power (1mW), narrow-linewidth (<10 MHz) probe that could be temperature tuned right across the grating's bandgap. The pump pulses, derived from a directly modulated DFB laser, were amplified to high power (20 kW) in an erbium doped fibre amplifier cascade based on large mode area erbium doped fiber and had a repetition frequency of 4kHz. The pump pulse shape was asymmetric due to gain saturation effects within the amplifier chain and exhibited a 30ps rise time and a 3ns half-width (see Fig. 5). Note that, as the optical pushbroom relies on the intensity gradient of the pump, the strength of our interaction is stronger than that which would be achieved using a transform limited pulse of the same FWHM and energy. The spectral half-width of the pulses at the grating input was measured to be 1.2GHz.

The pump and probe were polarization coupled into the FBG and were thus orthogonally polarised within the FBG. A half-wave plate was included within the system allowing us to orient

the beams along the grating birefringence axes. Both the

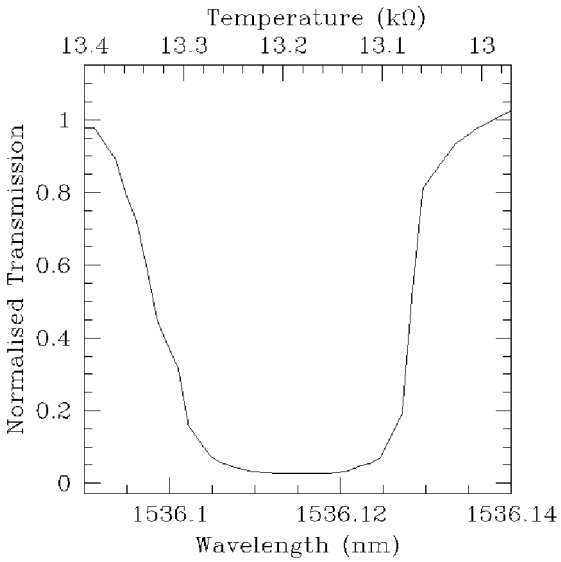

Figure 4: Measured reflection spectrum of the FBG used in the experiments. The wavelength resolution is 0.001nm. The horizontal scale gives the wavelength separation in nanometres from the centre wavelength of 1535.930nm. The dashed vertical line indicates the frequency of the probe for the results shown in Fig. 5

reflected and transmitted probe signals could be measured in our experimental system using a fiberized detection system based on a tunable, narrow-band (1nm) optical filter with greater than 80 dB differential loss between pump and probe (sufficient to extinguish the high intensity pump signal), a low noise pre-amplifier, a fast optical detector and sampling scope. The temporal resolution of our probe beam measurements was approximately 50ps.

The FBG was centered at 1535.93nm and was 8cm long with an apodised profile resulting in the suppression of the side-lobes. The grating had a peak reflectivity of 98% and a measured width of 32pm as shown in Fig. 4. In Fig. 4 the horizontal scale gives the difference in nanometres from the centre wavelength. The grating was mounted in a section of capillary tube and angle polished at both ends so as to eliminate reflections from the grating end faces and was appropriately coated to strip cladding modes.

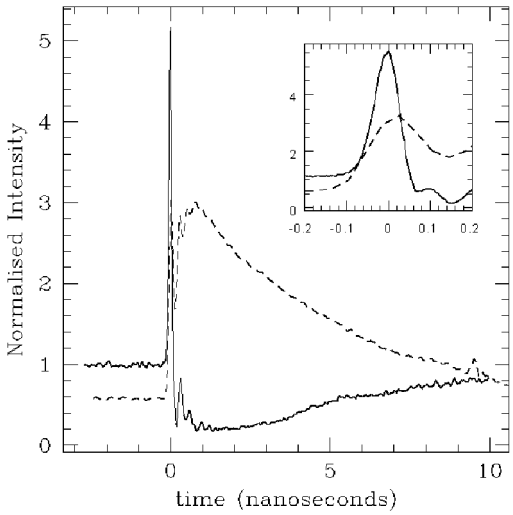

Figure 5: Experimental trace of the pushbroom. The solid line shows the intensity of the probe beam normalized so that the transmitted power in the absence of the grating would be unity. The dashed line shows the transmitted pump beam. The inset shows a expanded view of the front peak.

In Fig. 5 the optical pushbroom can be seen in action for the first time, the line styles and the insert are the same as for Fig. 2. The probe's wavelength is indicated by the dashed vertical line in Fig. 4. Note that it lies on the long wavelength side of the bandgap, where the linear transmission is close to 100%. This wavelength is indicated by the dashed vertical line in Fig. 4. The peak power of the pump within the FBG is set to 25kW. The transmitted probe is clearly seen to have developed a sharp (70ps FWHM) spike in intensity, co-located in time with the

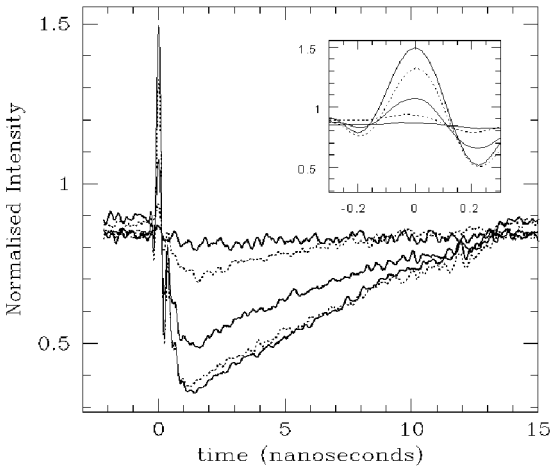

Figure 6: Experimental traces of the pushbroom with non-optimal parameters. In these cases the linear transmission is only 90% and the different traces show the effect of reducing the pump power. The peak pump powers used are 25kW, 22kW, 14kW, 6kW, 1kW. The increasing peak heights in the insert correspond to the increasing peak pump powers.

peak of the pump pulse. The transmission then drops well below unity for a considerable length of time - note that even 10ns after the arrival of the pump pulse the transmission has still not fully recovered. The parameters used in the numerical model in Fig. 2 match the actual experimental parameters, and as can be seen excellent agreement between the experimental and the numerical results is obtained.

We examined the dependence of the pushbroom on both the pump power and probe wavelength.

Fig. 6 shows some of these results. Compared to Fig. 5 we tuned the probe closer to the bandgap where the linear transmission was 90% and varied the pump power. It can be clearly seen that as the pump power decreases so does the quality of the pushbroom. This corresponds well to what we expect theoretically. Note that in Fig. 6 the peak transmission is less than twice that of the linear response as compared to a factor of five in the optimized system.

Conclusions

Compared to earlier experiments on nonlinear effects in FBG[1, 2, 4] these results are particularly clear. The main reason for this is that our gratings were centered near 1550nm which is one of the main telecommunications windows in optical fibres. This allowed us to make use of the various holographic techniques for writing good quality FBGs with arbitrary profiles developed for the communications industry. Similarly high quality fiberized components are readily available at these wavelengths making the optical pushbroom relatively simple to setup and observe. Lastly the latest generation of high-power fibre lasers operate in this region corresponding as it does to the gain peak of the Erbium doped fibre amplifier. Our results thus illustrate the potential of the powerful combination of versatile, high-power, erbium fiber sources with convenient, high-performance communication componentry and FBG fabrication technology for the study of the nonlinear optics of Bragg gratings. Indeed these results are probably the clearest manifestation of a nonlinear effects in a Bragg grating presented to date.

We have experimentally demonstrated the optical pushbroom effect for the first time. Using a strong pump beam we compressed a weak CW probe beam inside a Bragg grating, resulting in a narrow optical pulse at the output. Central to these results was the fact that in a Bragg grating the group velocity dispersion is many orders of magnitude higher than in an optical fibre, thus allowing nonlinear effects to be seen in short lengths of fibre. Furthermore this effect could be seen in any photonic crystal with a Kerr nonlinearity. Photonic crystals are perhaps the ideal structures to see nonlinear effects since the photonic band structures, and hence the dispersion, can be designed in order to see a particular effect such as the optical pushbroom.

Acknowledgments

This work is funded in part by the EPSRC ROPA project BRAGG. Two of us DJR and RIL would like to acknowledge the support of the Royal Society through the university research fellowship scheme.

References

1. U.Mohideen et al., Opt. Lett. 20, (1995).

2. B.J.Eggleton et al., Physical Review Letters 76, 1627 (1996).

3. H.G.Winful, J.H.Marburger, and E.Garmire, Applied Physics Letters 35, 379 (1979).

4. S.LaRochelle et al., Elect. Lett. 26, 1459 (1990).

5. C.M.de Sterke, Optics Letters 17, 914 (1992).

6. M.J.Steel and C.M.de Sterke, Physics Review A 49, 5048 (1994).

7. C.M.de Sterke et al., Optical Fiber Technology 2, 253 (1996).

8. C.M.de Sterke, N.G.Broderick, B.J.Eggleton and M.J.Steel,

9. M.J.Steel and C.M.de Sterke, Appl. Opt. 35, 3211 (1995).

10. H.He and P.D.Drummond, Phys. Rev. Lett. 78, 4311 (1997).